A Rational Design of Thin-Walled Pressure Vessel Ends[1]

W. Szyszkowski
Visiting Associate Professor.

P. G. Glockner
Professor and Head.

Department of Mechanical Engineering,
The University of Calgary,
Alberta, Canada

Optimal contours for heads of cylindrical pressure vessels are discussed. As opposed to the common method of preventing buckling in pressure vessel ends by means of increased wall thickness or local reinforcements, this paper proposes a design for "buckle-free" shapes in which the contour is established/adjusted so as to ensure stable behavior. A previous analysis by the authors, in which compressive stresses were eliminated, is extended so as to take into account the actual flexural rigidity of the wall. The shapes obtained from such buckle-free designs appear to be similar to standard ellipsoidal and torispherical ends and should be acceptable from various design and aesthetic viewpoints.

1 Introduction

Cylindrical pressure vessels are usually closed by axisymmetric end elements the shapes of which are chosen on the basis of fabrication and strength requirements. From a fabrication/production viewpoint, the end should be as shallow as possible, while stress analysis suggests a higher contour for the head so as to result in a smooth membrane stress transition from the end to the cylinder while, at the same time, also minimizing bending effects at their juncture. The simplest end for a cylindrical pressure vessel, from a fabrication viewpoint, is a flat plate. Unfortunately, stresses in such a plate element as well as the bending stresses at its juncture to the cylinder are unacceptably high. Consequently, spherical or ellipsoidal pressure vessel ends are normally used. For example, the hemispherical closure shows favorable stress distribution and minimal bending effects at the juncture, but its fabrication may present problems. Between the flat plate and the hemispherical closure, representing the two "extremes" in shapes, there are "compromise" contours, including ellipsoidal and torispherical ends, which are recommended by standard codes [1]. Particularly common shapes used in practice include the 2:1 ellipsoidal and the torispherical heads, with a radii ratio for the latter of $R_s = 2R_c$ (see Fig. 1), shapes for which the membrane stress resultants in the apex region are equal to the maximum "circumferential" membrane stress resultants in the cylinder, thereby permitting use of the same wall thickness throughout the pressure vessel.

The effectiveness of these "standard" ends has been verified by countless applications for small pressure vessels. When such heads are used on large pressure vessels for which the diameter/thickness ratio, D/t, is relatively large ($(D/t) > 700$ [2]), difficulties are encountered in terms of wrinkling in the compressive stress zone, a phenomenon which can easily be explained on the basis of a simple membrane stress analysis, typical examples for which are given on Figs. 1(*b*) and (*c*) for the 2:1 ellipsoidal and the torispherical ($R_s = 2R_c$) ends, respectively. Both figures indicate regions of circumferential compressive stresses which obviously become dangerous in the case of thin-walled structures and are responsible for such local buckling. Even though such local instability does not represent total failure, as one would normally expect in the case of buckling due to external pressure, the appearance of wrinkles may interfere with the use/function of the vessel and could even lead to local fracturing in the vicinity of the buckles [2]. Numerous investigations have been carried out in recent past, studies which were directed at gaining a better understanding of this phenomenon and finding methods for the prevention of such local buckling. The main purpose of most of these investigations, however, was to establish safe internal pressure ranges for standard ellipsoidal or torispherical pressure vessel ends. Experimental [3, 4] and numerical [5–10] studies revealed the complexity of this type of behavior of the vessel ends, behavior in which geometrical and material nonlinearities interact and play a significant role. A review of this problem was presented in [2], where approximate simple formulas defining the critical internal pressure were also given.

The most commonly used method for ensuring stability in pressure vessel closures is to either increase the wall thickness or to apply local reinforcements (stringers) in regions of compressive stresses, thereby increasing the bending stiffness of the wall in such regions. Such preventive measures lead to structures in which some portion of the material is sacrificed exclusively for prevention of instability. In that sense, such structures are not "optimal."

In the method of design for "safe ends," presented here, instead of designing for bending stiffness to prevent buckling, the shape of the pressure vessel head is corrected so as to reduce the compressive membrane forces to allowable/controlled levels. Consequently, such "corrected shapes" ensure buckle-free behavior. In addition, in such contours the entire strength of the material is available for carrying internal

[1]The results presented here were obtained in the course of research sponsored by the Natural Sciences and Engineering Research Council of Canada, Grant No. A-2736.

Contributed by the Pressure Vessels and Piping Division for publication in the JOURNAL OF PRESSURE VESSEL TECHNOLOGY. Manuscript received by the PVP Division; January 8, 1986.

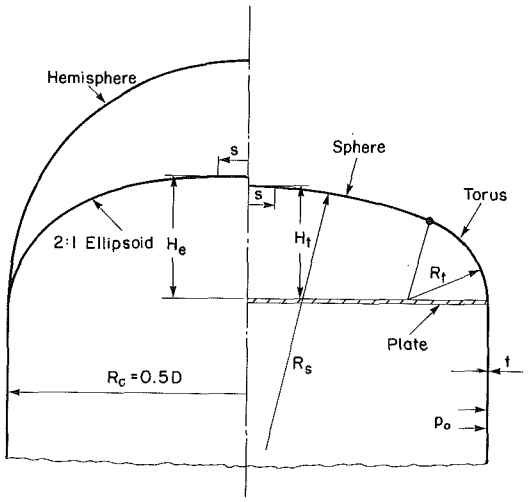

(a) Some end profiles

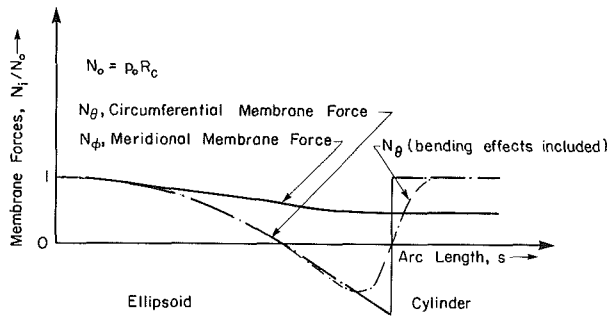

(b) Membrane force distribution for 2:1 ellipsoidal end

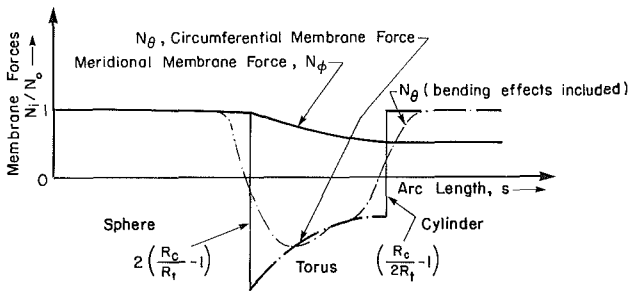

(c) Membrane force distribution for torispherical end

Fig. 1 Typical ends of cylindrical pressure vessels

pressure. Buckle-free shapes were introduced in [11, 12], where only tensile membrane stress states were allowed. In the present work, such designs are relaxed and further improved by taking into account the actual compressive stiffness of the wall and permitting some "controlled" circumferential compressive membrane force.

The shapes obtained from these buckle-free designs, though quite similar to the shapes of standard vessel ends, have significantly different curvatures. Special attention needs to be paid therefore in the manufacturing of such vessel closures. The shape correction is based primarily on the membrane stress state. However, bending stresses are calculated for the "final shapes," which due to the reduced discontinuities in the membrane stress state, are found to be smaller than the flexural stresses in typical pressure vessel ends. Such reduced bending stresses at the juncture of the vessel end and the cylindrical portion may be a further design advantage, particularly when the pressure vessel is subjected to cyclic loading and/or is made of brittle materials.

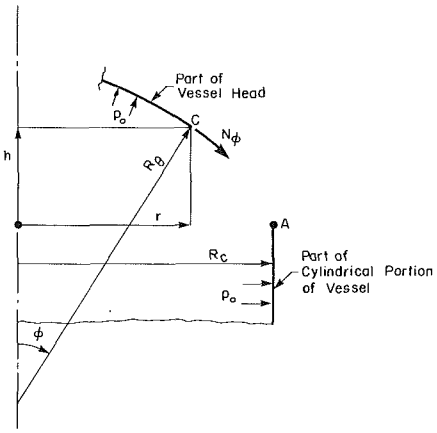

Fig. 2 Notation and coordinate system

2 Tension-Only Heads

Since under internal pressure loading, the meridional stress resultant, N_ϕ, is tensile, we are looking for a shape in which the circumferential stress, N_θ is, at worst, zero, this case representing the boundary between the desirable tensile, and the unacceptable compressive stress state. The governing equations for shapes of this type subjected to arbitrary loading conditions were discussed in [12]. For the case of the constant internal pressure, p_o, the shape is readily determined from the static equilibrium equations for such structures, written in the form

$$N_\phi = \frac{p_o r}{2\sin\phi} = \frac{p_o R_\theta}{2}; \quad \frac{N_\phi}{R_\phi} = p_o \qquad (1a,b)$$

where R_ϕ and R_θ denote radii of meridional and circumferential curvatures, respectively, r and ϕ are coordinates (see Fig. 2) and N_θ is assumed to vanish. From equations (1), one obtains

$$R_\theta = 2R_\phi \qquad (2)$$

Using the geometric relations

$$R_\theta = \frac{r}{\sin\phi}; \quad R_\phi = \frac{1}{\cos\phi}\frac{dr}{d\phi} \qquad (3a,b)$$

in equation (2), leads to

$$\frac{dr}{d\phi} = \frac{r}{2}\cot\phi \rightarrow r(\phi) = C_o\sqrt{\sin\phi} \qquad (4a,b)$$

where C_o represents a constant of integration.

The shape defined by equation (4) has to be joined to the cylindrical portion of the vessel; therefore,

$$r\left(\frac{\pi}{2}\right) = R_c \quad \therefore\ C_o = R_c$$

allowing determination of all parameters as functions of the angle ϕ in the form

$$\bar{r} = \sqrt{\sin\phi}; \qquad \bar{h} = \frac{1}{2}\int_\phi^{\pi/2}\sqrt{\sin\phi}\,d\phi \qquad (5a,b)$$

$$\bar{R}_\phi = \frac{1}{2\sqrt{\sin\phi}}; \qquad \bar{R}_\theta = \frac{1}{\sqrt{\sin\theta}}; \qquad (5c,d)$$

$$\bar{N}_\phi = \frac{1}{2\sqrt{\sin\phi}}; \qquad \bar{N}_\theta = 0 \qquad (5e,f)$$

where h is the height coordinate shown in Fig. 2 and $\bar{r} = r/R_c$, $\bar{h} = h/R_c$, $\bar{R}_i = R_i/R_c$, $\bar{N}_i = N_i/(p_o R_c)$ $(i = \phi, \text{or } \theta)$. Since the variable $\bar{h}$ is expressed in the form of an integral, a numerical treatment is required, in general, for its evaluation.

Table 1 Coordinates for buckle-free shape

ϕ	$\bar{r}$	$\bar{h}$ (exact)	$\bar{h}$ (from equation 6)	$\bar{h}$ (from equation 7)
0	0	0.5991	0.5991	0.6239
10	0.4167	0.5748	0.5748	0.5847
20	0.5848	0.5306	0.5306	0.5349
30	0.7071	0.4740	0.4740	0.4757
40	0.8017	0.4080	0.4080	0.4086
50	0.8752	0.3347	0.3347	0.3349
60	0.9360	0.2558	0.2559	0.2558
70	0.9694	0.1728	0.1730	0.1728
80	0.9924	0.0870	0.0874	0.0870
90	1.0000	0.0000	0.0007	0.0000

An approximate closed-form solution can be obtained by rearranging equation (5*b*) as

$$\bar{h}=\frac{1}{2}\left[\int_0^{\pi/2}\sqrt{\sin\phi}\,d\phi-\int_0^{\phi}\sqrt{\sin\phi}\,d\phi\right]$$

$$=I-\frac{1}{2}\int_0^{\phi}\sqrt{\sin\phi}\,d\phi \qquad (6a)$$

where

$$I=\frac{\Gamma\left(\frac{3}{4}\right)\cdot\Gamma\left(\frac{1}{2}\right)}{4\,\Gamma\left(\frac{5}{4}\right)}=0.55907$$

and where Γ denotes the Gamma function. Expanding the remaining intergral in equation (6*a*) into a Taylor series, one obtains

$$\bar{h}\ (\phi)\cong I-\frac{1}{3}\,\phi^{3/2}\left(1-\frac{1}{28}\,\phi^2\right) \qquad (6b)$$

which approximates the exact relation (equation (6*a*)) with surprising accuracy over the full range of ϕ (see Table 1). For a better approximation in the vicinity of the junction between the vessel end and the cylinder, one could use the relation

$$\bar{h}(\phi)=\frac{1}{2}\left(\frac{\pi}{2}-\phi\right)\cdot\left[1-\frac{1}{12}\left(\frac{\pi}{2}-\phi\right)^2\right] \qquad (7)$$

From equations (5*a*, *c*, *d*) it is clear that the curvatures of the vessel end are proportional to the distance $\bar{r}$ resulting in a very flat contour in the vicinity of the apex. Expression (5*e*) indicates that the membrane stress resultant $\bar{N}_\phi \to \infty$ at the apex. However, the standard vessel ends perform quite satisfactorily in this region and can therefore be used as the central portion of the closure. Thus, the main purpose of this paper is to describe and define a correction to the standard ends in the regions of compressive membrane forces. Such a correction of the torispherical contour is shown in Fig. 3(*a*). All parameters associated with such a corrected buckle-free shape are denoted by a sub/superscript *b*. The original torispherical contour is denoted in Fig. 3 by the sub/superscript *t*. The juncture between the central (spherical) portion and the outer buckle-free shape, defined by point B in Fig. 3(*a*), is determioned by means of the equations

$$\bar{r}_B=\sqrt{\sin\phi_B}=\bar{R}_s\,\sin\phi_B;\ \therefore\ \sin\phi_B=\frac{1}{\bar{R}_s^2} \qquad (8)$$

The torispherical end with $\bar{R}_t = R_t/R_c = 0.4$ is also shown on Fig. 3(*a*). Although the two contours are quite similar, the meridional curvatures of the buckle-free shape are almost twice those of the torispherical contour (see Fig. 3(*b*)). This difference in curvature affects the membrane force distribution significantly, as indicated in Fig. (3*c*), a distribution which was calculated on the basis of the standard "edge-effect" bending solution. Note also that for the buckle-free shape the membrane stress state is tensile, with $\bar{N}_\theta^b$ vanishing in most of the region AB, while the torispherical contour exhibits large compressive hoop membrane effects, with sharp gradients, in the same region, which may necessitate a geometrically nonlinear analysis in that zone [7]. The only disadvantage of the buckle-free shape shown on Fig. 3(*a*), is its height $H_b = 0.620\,R_c$ as compared with the corresponding value for the torispherical end $H_t = 0.517\,R_c$.

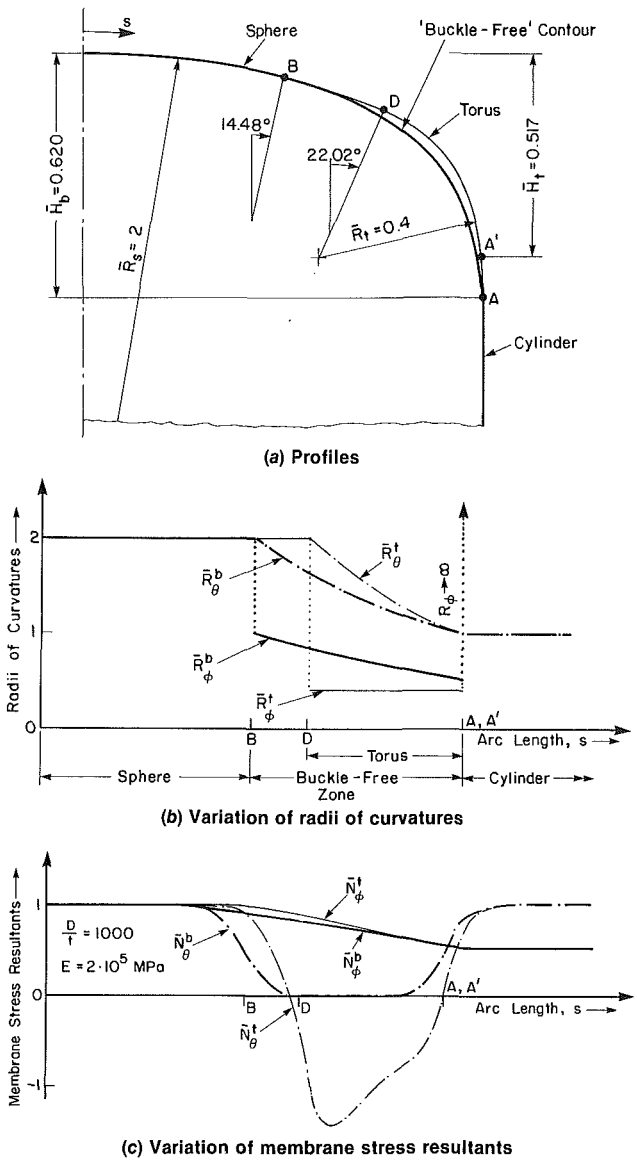

Fig. 3 Corrected torispherical shape

The buckle-free correction for the 2:1 ellipsoidal end is shown on Fig. 4(*a*). The location of the juncture, point B, is found from the relation

$$\bar{r}_e=\frac{2\,\sin\phi_B}{\sqrt{1+3\,\sin^2\phi_B}}=\bar{r}_b=\sqrt{\sin\phi_B};\ \therefore\ \sin\phi_B=\frac{1}{3} \qquad (9)$$

As can be seen, the "correction" is now even smaller than in the torispherical case. Nevertheless, the differences in curvatures between the original and the corrected contour are quite substantial (see Fig. 4(*b*)), leading to significant differences in hoop membrane stress distributions, the shape correction again eliminating what was a sizeable compressive membrane stress zone (see Fig. 4(*c*)). The corrected shape has a height $H_b = 0.620\,R_c$, which is approximately the same as

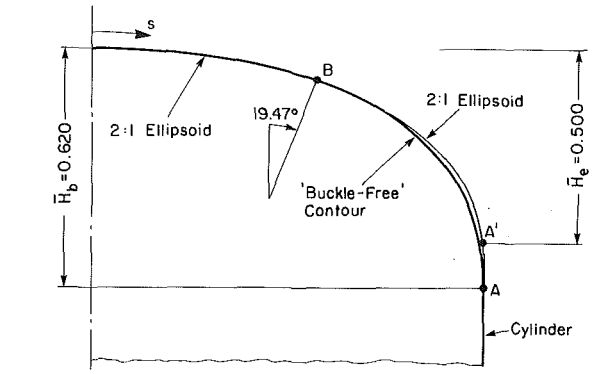

(a) Profiles

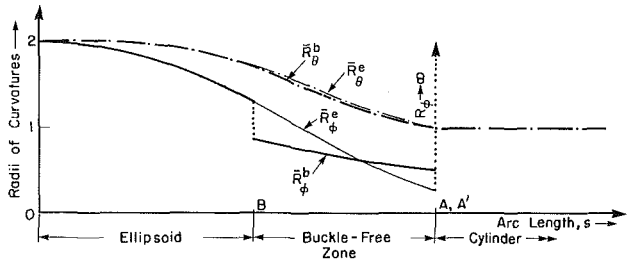

(b) Variation of radii of curvatures

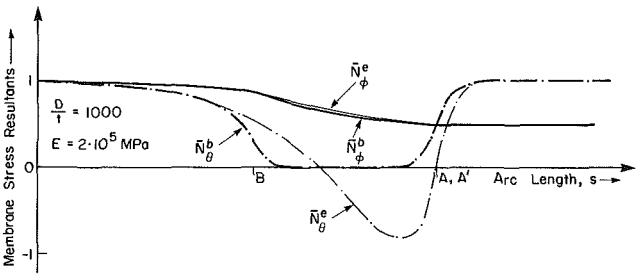

(c) Variation of membrane stress resultants

Fig. 4 Corrected ellipsoidal shape

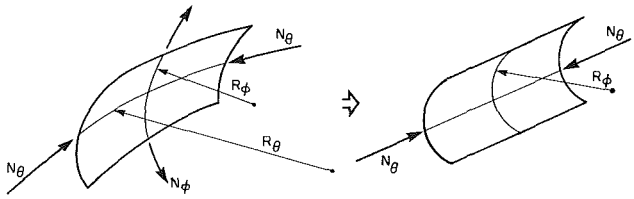

(a) Doubly curved and corresponding cylindrical panel

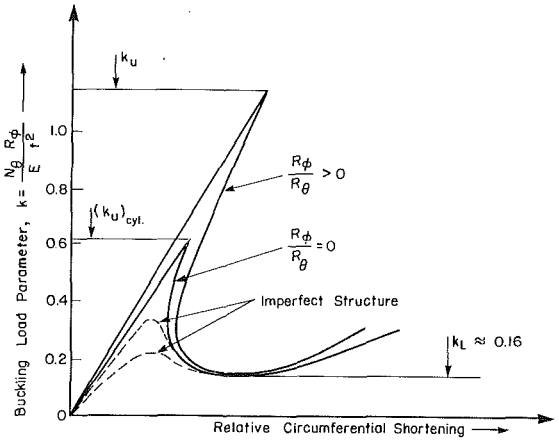

(b) Load-deflection characteristics of doubly and singly curved panels (from [13])

Fig. 5 Stability behavior of shell elements

that of the buckle-free contour for the torispherical case, while the original elliptical contour is slightly lower, $H_e = 0.500\,R_c$.

An examination and comparison of Figs. 3 and 4 also reveals that in the uncorrected (torispherical and ellipsoidal) shapes there are nonzero meridional and hoop membrane forces of opposite sign in the region of high curvature, a membrane stress state which is much more conducive to initiation of yielding than the corresponding stress state for the buckle-free shapes in which the hoop membrane force vanishes in the same region. Thus, the shape correction proposed here allows further optimization of the design leading to a more uniform stress distribution throughout the vessel end.

3 Heads With Controlled Compressive Membrane Forces

Pressure vessel closures made of metal have a finite thickness and some (nonzero) bending rigidity. Consequently, they can carry some compressive membrane forces. Determination of the allowable membrane compressive stress at each point in the vessel end is, in general, a complex problem. A conservative estimate can be obtained, however, by assuming that the compressive stiffness of the doubly curved vessel depends only on the meridional curvature of the contour, thus, in effect, approximating the doubly curved shape by a corresponding cylindrical panel (see Fig. 5(*a*)). The stability of such a doubly curved surface element was discussed in [13] with some of the results shown in Fig. 5(*b*)). As there results indicate, the circumferential curvature ($R_\theta^{-1} > 0$) increases the nondimensional bifurcation buckling load parameter, k_u, significantly, while the lowest post-buckling load-carrying capacity, k_L, is unaffected by this parameter, indicating that the doubly-curved element and the corresponding cylindrical panel have approximately the same postbuckling strength. Figure 5 (*b*) also indicates the high imperfection sensitivity of these types of surface elements and the fact that the limit load for the imperfect structure is always larger than the minimum post-buckling strength, k_L, of the perfect structure.

On the basis of the above stated approximation, one can conservatively assume the allowable circumferential compressive membrane force to be restricted by

$$\frac{|N_\theta|}{Et_b}\,\frac{R_\phi}{t_b} \le k_L \tag{10}$$

where E is Young's modulus, $k_L \cong 0.16$ and t_b denotes the wall thickness of the buckle-free shape. On the basis of data presented in [2], the bifurcation buckling load parameter, k_u, was calculated for the 2:1 ellipsoidal and the torispherical heads indicating values for this parameter in the ranges 0.7–1.1 and 0.8–1.5 for these shapes, respectively. These ranges are above the single k_u value of 0.605 calculated for the corresponding cylindrical panels and certainly are much higher than the minimum post-buckling strength, k_L. Thus these results, justify, in some sense, the use of the foregoing assumption and equation (10).

Using equation (10), one can admit circumferential membrane stress resultants in magnitude given by

$$N_\theta = -k_L\,E\,\frac{t_b^2}{R_\phi} \tag{11}$$

Since N_ϕ is given by equation (1*a*) and the radii of curvatures are defined by equations (3*a*,*b*), these expressions used in the equation of equilibrium for the surface normal direction leads to

$$\frac{N_\theta}{R_\theta}+\frac{N_\phi}{R_\phi}=p_o;\ \therefore\ \frac{d\bar{r}}{d\phi}=\frac{\bar{r}}{2}\cot\phi - c\,\sin 2\phi/r \tag{12a,b}$$

where

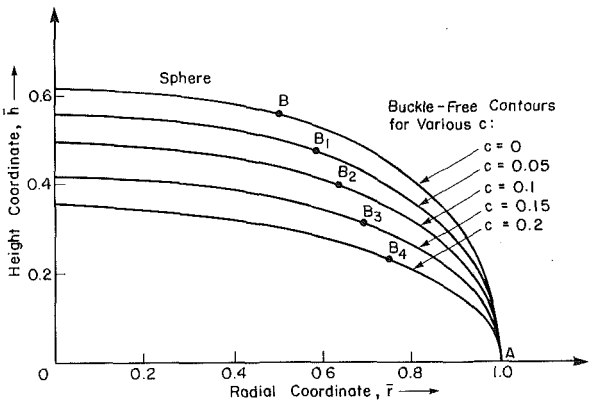

Fig. 6 Variation of buckle-free profiles with c

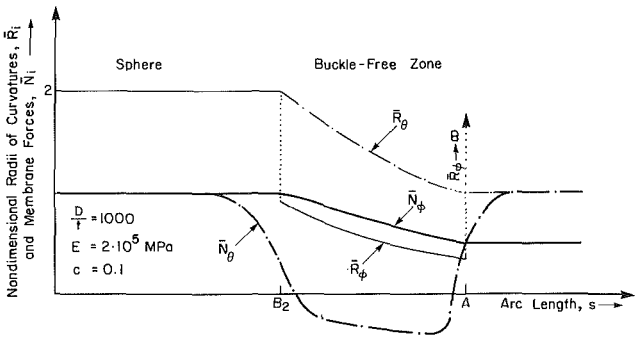

Fig. 7 Variation of curvature and membrane stress resultants in buckle-free design for c = 0.1

$$c=\frac{k_L}{2}\frac{E}{p_o}\left(\frac{t_b}{R_c}\right)^2 \tag{12c}$$

Integrating equation (12*b*) and using the boundary condition $\bar{r}(\pi/2) = 1$ leads to

$$\bar{r}\ (\phi)=\sqrt{\sin\phi[1+4c(1-\sin\phi)]} \tag{13}$$

which reduces to equation (5*a*) for $k_L \to 0$. The second (height) coordinate is expressed in the form

$$\bar{h}=\frac{1}{2}\int_{\phi}^{\pi/2}\sqrt{\sin\phi}\left[\frac{1+4c(1-2\sin\phi)}{[1+4c(1-\sin\phi)]^{1/2}}\right]d\phi \tag{14}$$

while the remaining parameters are obtained in the form

$$\bar{R}_\phi = \frac{1}{2}[1+4c\,(1-2\sin\phi)]/\bar{r} \tag{15a}$$

$$R_\theta = \bar{r}/\sin\phi \tag{15b}$$

$$N_\phi = \bar{r}/(2\sin\phi);\ \bar{N}_\theta = -2c/\bar{R}_\phi \tag{15c,d}$$

The calculated buckle-free profiles for various values of c are shown on Fig. 6. The central portion of the head is again assumed to be spherical with $R_s = 2R_c$. The parameters defining the juncture between the spherical and the corrected shape portions, points B_i, are given by

$$\bar{r}_B=\frac{1}{2}\frac{1+4c}{1+c};\ \sin\phi_B=\frac{1+4c}{4+4c}=\frac{1}{2}\bar{r}_B \tag{16a,b}$$

As can be observed from Fig. 6, the height of the closure decreases with increasing c, a parameter which depends on the internal pressure, p_o. If one assumes p_o to be a function of the allowable membrane stress in the spherical and cylindrical portions of the vessel, both of which have wall thickness t, the pressure is expressed as

$$p_o=\sigma_{all}\frac{t}{R_c} \tag{17}$$

which when substituted into equation (12*c*) leads to

$$c\frac{k_L}{2}\frac{E}{\sigma_{all}}\cdot\frac{t}{R_c}\left(\frac{t_b}{t}\right)^2 \tag{18}$$

For steels generally used in pressure vessel production, the order of magnitude of some of these parameters is given by $E/\sigma_{all} = O(10^3)$; $t/R_c = O(2.0\times10^{-3})$; assuming further that $t_b = t$, one arrives at $c = O(k_L)$.

Finally, the variation of curvatures and membrane stress resultants for a closure with $c = 0.1$ is given on Fig. 7. This diagram indicates the presence of a circumferential compression zone which, in comparison with the corresponding compressive stress area for the 2:1 ellipsoidal head of approximately the same height, is larger and exhibits a smoother N_θ distribution with maximum values of this stress variable also reduced substantially.

From an optimal design viewpoint, one strives for a membrane stress distribution in the vessel which is as uniform as possible. In order to ensure uniform membrane strength (against yielding) for all portions of the vessel and since for the spherical and cylindrical portions max $(\bar{N}_\phi - \bar{N}_\theta) = 1$, the stress resultants must satisfy the following condition in the buckle-free shape:

$$(\bar{N}_\phi - \bar{N}_\theta) \approx 1 \tag{19}$$

An analysis of the membrane stress resultants, including bending effects, for $0 < c < 0.2$ indicates that

$$(\bar{N}_\phi - \bar{N}_\theta)_{max} \cong \max\left[1;\ \frac{1+2c}{2(1-4c)}\right] \tag{20}$$

which suggests that condition (19) is approximately satisfied provided

$$\frac{1+2c}{2(1-4c)} \approx 1;\ \therefore\ c \approx 0.1 \tag{21}$$

Figure 7 indicates the validity of equation (19) in the zone of compressive stresses thereby confirming the optimal design of the closure with a value of $c = 0.1$. For $c < 0.1$ the buckle-free shape would be "understressed," as for example the heads shown on Figs. 3 and 4, while for $c > 0.1$ the compressive membrane forces will become higher leading to possible premature plastification. The meridional (tensile) membrane stress resultants are almost totally insensitive to the variation in c. One should note that the discussion concerning stability of the compressive region of the closure was based on equation (11), and therefore does not include plastic deformations or plastic buckling. If one requires or desires a vessel end with low height, Fig. 6 indicates that in such cases $c > 0.1$ which, in turn, suggests an increase in wall thickness in the buckle-free zone, $t_b > t$.

Conclusions

In the design approach for pressure vessel ends presented here, the circumferential compressive membrane stress resultants are either completely eliminated or effectively controlled. In the first case, the corrected portion of the closure, referred to as the buckle-free zone, is slightly understressed from a optimal design point of view and leads to heads with relatively large heights. Admitting some circumferential compression allows shallower profiles and results in almost uniform membrane strength throughout the pressure vessel end, signifying an optimal design.

The analysis indicates that such buckle-free shapes are obtained by relatively small corrections of the commonly used profiles, corrections which, however, have substantial meridional curvature changes associated with them. Consequently, even such small corrections require properly shaped dyes for the reforming and reshaping of the standard profiles.

What does buckle-free really mean? Consider a standard

closure for a pressure vessel, subjected to internal pressure. At a certain pressure level wrinkling may occur in the compressive zone of the head. The wrinkled profile would tend to move "inward," resulting in a reduction in the circumferential compressive membrane forces. The final "average" wrinkled, (deflected) geometry, discussed in [14], is a good first approximation for the buckle-free profile discussed in this paper. Thus, wrinkling may, in some sense, be considered as the structure's self-defence against design deficiencies. Indeed, the post-buckling average profile determined experimentally might be utilized to define contours approaching the buckle-free shape. Naturally, we are not suggesting that wrinkled pressure heads are proper closures for high-pressure containment vessels, nor are we suggesting that buckle-free shapes be determined experimentally. On the contrary, we believe that the analysis presented here provides an effective and economical method for establishing contours resulting in buckle-free behavior.

References

1 Megyesy, E. F., *Pressure Vessel Handbook*, Fifth Edition, Pressure Vessel Handbook Publish Inc., Tulsa, 1981.

2 Galletly, G. D., "Buckling and Collapse of Thin Internally-Pressurized Dished Ends," *Proceedings of the Institute of Civil Engineers*, Vol. 67, Part 2, 1979, pp. 607–626.

3 Kirk, A., and Gill, S. S., "The Failure of Torispherical Ends of Pressure Vessels Due to Instability and Plastic Deformation – An Experimental Investigation," *International Jouranl of Mechanical Science*, Vol. 17, 1975, pp. 525–544.

4 Patel, P. R., and Gill, S. S., "Experiments on the Buckling Under Internal Pressure of Thin Torispherical Ends of Cylindrical Pressure Vessels," *International Journal of Mechanical Science*, Vol. 20, 1978, pp. 159–175.

5 Brown, K. W., and Kraus, H., "Stability of Internally Pressurized Vessels with Ellipsoidal Heads," ASME JOURNAL OF PRESSURE VESSEL TECHNOLOGY, Vol. 98, 1976, pp. 157–161.

6 Bushnell, D., and Galletly, G. D., "Stress and Buckling of Internally Pressurized Elastic-Plastic Torispherical Vessel Heads – Comparisons of Test and Theory," ASME JOURNAL OF PRESSURE VESSEL TECHNOLOGY, Vol. 99, 1977, pp. 39–53.

7 Bushnell, D., "Nonsymmetric Buckling of Internally Pressurized Ellipsoidal and Torispherical Elastic-Plastic Pressure Vessel Heads," ASME JOURNAL OF PRESSURE VESSEL TECHNOLOGY, Vol. 99, 1977, pp. 54–63.

8 Kanodia, V. L., Gallagher, R. H., and Mang, H. A., "Instability Analysis of Torispherical Pressure Vessel Heads with Triangular Thin-Shell Finite Element," ASME JOURNAL OF PRESSURE VESSEL TECHNOLOGY, Vol. 99, 1977, pp. 64–74.

9 Galletly, G. D., and Aylward, R. W., "Plastic Collapse and the Controlling Failure Pressures of Thin 2:1 Ellipsoidal Shells Subjected to Internal Pressure," ASME JOURNAL OF PRESSURE VESSEL TECHNOLOGY, Vol. 101, 1979, pp. 64–72.

10 Galletly, G. D., and Radhamohan, S. K., "Elastic-Plastic Buckling of Internally Pressurized Thin Torispherical Shells," ASME JOURNAL OF PRESSURE VESSEL TECHNOLOGY, Vol. 101, 1979, pp. 216–225.

11 Mansfield, E. H., "An Optimum Surface of Revolution for Pressurized Shells," *International Journal of Mechanical Science*, Vol. 23, 1981, pp. 57–62.

12 Szyszkowski, W., and Glockner, P. G., "Design for Buckle-Free Shapes in Pressure Vessels," ASME JOURNAL OF PRESSURE VESSEL TECHNOLOGY, Vol. 107, 1985, pp. 387–393.

13 Lukasiewicz, S., and Szyszkowski, W., "On the Stability and the Post-Buckling Equilibrium of Shells of Revolution," *ZAMM*, Vol. 51, 1971, pp. 635–639.

14 Szyszkowski, W., "The Analysis of Adaptation Possibilities of Some Axisymmetrical Shells After Local Buckling," *Mechanica Teoretyczna i Stosowana*, Vol. 16, 1978, pp. 557–571.